5

ELECTRON EMISSION SPECTROSCOPIES

5.0   INTRODUCTION

In this chapter we have collected together those techniques in which one measures the energy distribution of electrons ejected from a material. In all four techniques covered electronic energy level excitations are involved, providing atomic or chemical state identification, or both. All are also true surface techniques, since the energies of the electrons concerned fall in the range where they travel can only very short distances without being inelastically scattered. These techniques are all sensitive to less than monolayer amounts of material and none have probing depths greater than about 50 Å without using sputter profiling.

The first two techniques discussed, X-Ray Photoelectron Spectroscopy, XPS, (also known as Electron Spectroscopy for Chemical Analysis, ESCA) and Ultraviolet Photoelectron Spectroscopy, UPS, are very closely related. XPS involves soft X rays (usually 1486 eV, from an Al anode) ejecting photoelectrons from the sample. Electrons originating from the core levels identify the elements present from their Binding Energies, BE. Small "chemical shifts" in the BEs provide additional chemical state information. The relative concentrations of the different elements present can be determined from relative peak intensities. XPS identifies all elements except hydrogen and helium from a depth ranging from around 2 monolayers to 25 monolayers. Typical values for XPS peaks in the 500–1400 eV kinetic energy range are 5 to 10 monolayers.

The strengths of XPS are its good quantification, its excellent chemical state determination capabilities, its applicability to a wide variety of materials from biological materials to metals, and its generally nondestructive nature. XPS's weaknesses are its lack of good spatial resolution (70 μm), only moderate absolute sensitivity (typically 0.1 at. %), and its inability to detect hydrogen. Commercial XPS instruments are usually fully UHV compatible and equipped with accessories, including a sputter profile gun. Costs vary from $250,000 to $600,000, or higher if other major techniques are included.

UPS differs from XPS only in that it uses lower energy radiation to eject photoelectrons, typically the 21.2-eV and 40.8-eV radiation from a He discharge lamp, or up to 200 eV at synchrotron facilities. The usual way to perform UPS is to add a He lamp to an existing XPS system, at about an incremental cost of $30,000. Most activity using UPS is in the detailed study of valence levels for electronic structure information. For materials analysis it is primarily useful as an adjunct to XPS to look at the low-lying core levels that can be accessed by the lower energy UPS radiation sources. There are several advantages in doing this: a greater surface sensitivity because the electron kinetic energies are lower, better energy resolution because the source has a narrower line width, and the possibility of improved lateral resolution using synchrotron sources.

Auger Electron Spectroscopy, AES, is also closely related to XPS. The hole left in a core level after the XPS process, is filled by an electron dropping from a less tightly bound level. The energy released can be used to eject another electron, the Auger electron, whose energy depends only on the energy levels involved and not on whatever made the initial core hole. This allows electrons, rather than X rays, to be used to create the initial core hole, unlike XPS. Since all the energy levels involved are either core or valence levels, however, the type of information supplied, like XPS, is elemental identification from peak positions and chemical state information from chemical shifts and line shapes. The depths probed are also similar to XPS. Dedicated AES systems for materials analysis, which are of similar cost to XPS instruments, have electron optics columns producing finely focused, scannable electron beams of up to 30 kV energy and beam spot sizes as small as 200 Å, a great advantage over XPS. AES could have been discussed in Chapter 3 along with STEM, EMPA, etc. When the incident beam is scanned over the sample (Scanning Auger Microprobe, SAM) mapping at high spatial resolution is obtained. For various reasons the area analyzed is always larger than the spot size, the practical limit to SAM being in the 300–1000 Å range. Another advantage of AES over XPS is speed, since higher electron beam currents can be used. There are major disadvantages to using electrons, however. Beam damage is often severe, particularly for organics, where desorption or decomposition often occurs under the beam. Sample charging for insulators is also a problem. Overall, the two techniques are about equally widespread and are the dominant methods for nontrace level analysis at surfaces. AES is the choice for inorganic systems where high spatial resolution is needed (e.g., semi-

conductor devices) and XPS should be one's choice otherwise. Combined systems are quite common.

Reflected Electron Energy-Loss Spectroscopy, REELS, is a specialized adjunct to AES, just as UPS is to XPS. A small fraction of the primary incident beam in AES is reflected from the sample surface after suffering discrete energy losses by exciting core or valence electrons in the sample. This fraction comprises the electron energy-loss electrons, and the values of the losses provide elemental and chemical state information (the Core Electron Energy-Loss Spectra, CEELS) and valence band information (the Valence Electron Energy-Loss Spectra, VEELS). The process is identical to the transmission EELS discussed in Chapter 3, except that here it is used in reflection, (hence REELS, reflection EELS), and it is most useful at very low beam energy (e.g., 100 eV) where the probing depth is at a very short minimum (as in UPS). Using the rather high-intensity VEELS signals, a spatial resolution of a few microns can be obtained in mapping mode at 100-eV beam energy. This can be improved to 100 nm at 2-keV beam energy, but the probing depth is now the same as for XPS and AES. Like UPS, VEELS suffers in that there is no direct elemental analysis using valence region transitions, and that peaks are often overlapped. The technique is free on any AES instrument and has been used to map metal hydride phases in metals and oxides at grain boundaries at the 100-nm spatial resolution level.

5.1 XPS

X-Ray Photoelectron Spectroscopy

C. R. BRUNDLE

Contents

- Introduction
- Basic Principles
- Analysis Capabilities
- More Complex Effects
- Surface Sensitivity
- Instrumentation
- Applications
- Comparison with Other Techniques
- Conclusions

Introduction

The photoelectric process, discovered in the early 1900s, was developed for analytical use in the 1960s, largely due to the pioneering work of Kai Siegbahn's group.[1] Important steps were the development of better electron spectrometers, the realization that electron binding energies were sensitive to the chemical state of the atom, and that the technique was surface sensitive. This surface sensitivity, combined with quantitative and chemical state analysis capabilities have made XPS the most broadly applicable general surface analysis technique today. It can detect all elements except hydrogen and helium with a sensitivity variation across the periodic table of only about 30. Samples can be gaseous, liquid, or solid, but the vast majority of electron spectrometers are designed to deal with solids. The depth of the solid material sampled varies from the top 2 atomic layers to 15–20 layers. The area examined can be as large as 1 cm × 1 cm or as small as 70 μm × 70 μm (10-μm diam-

eter spots may be achieved with very specialized equipment). It is applicable to biological, organic, and polymeric materials through metals, ceramics, and semiconductors. Smooth, flat samples are preferable but engineering samples and even powders can be handled. It is a nondestructive technique. Though there are some cases where the X-ray beam damage is significant (especially for organic materials), XPS is the least destructive of all the electron or ion spectroscopy techniques. It has relatively poor spatial resolution, compared to electron-impact and ion-impact techniques. It is also not suitable for trace analysis, the absolute sensitivity being between 0.01–0.3% at., depending on the element. XPS can be a slow technique if the extent of chemical detail to be extracted is large. Analysis times may vary from a few minutes to many hours.

There are thousands of commercial spectrometers in use today in materials analysis, chemistry, and physics laboratories. The largest concentrations are in the US and Japan. They are used in universities, the semiconductor and computer industries, and the oil, chemical, metallurgical, and pharmaceutical industries.

Instruments combining XPS with one or more additional surface techniques are not uncommon. Such combinations use up relatively little extra space but cost more.

Basic Principles

Background

A photon of sufficiently short wavelength (i.e., high energy) can ionize an atom, producing an ejected free electron. The kinetic energy KE of the electron (the photoelectron) depends on the energy of the photon $h\nu$ expressed by the Einstein photoelectric law:

$$KE = h\nu - BE \tag{1}$$

where BE is the binding energy of the particular electron to the atom concerned. All of photoelectron spectroscopy is based on Equation (1). Since $h\nu$ is known, a measurement of KE determines BE. The usefulness of determining BE for materials analysis is obvious when we remember the way in which the electron shells of an atom are built up. The number of electrons in a neutral atom equals the number of protons in the nucleus. The electrons, arranged in orbitals around the nucleus, are bound to the nucleus by electrostatic attraction. Only two electrons, of opposite spin, may occupy each orbital. The energy levels (or eigenvalues ε) of each orbital are discrete and are different for the same orbital in different atoms because the electrostatic attraction to the different nuclei (i.e., to a different number of protons) is different. To a first approximation, the BE of an electron, as determined by the amount of energy required to remove it from the atom, is equal to the ε value (this would be exactly true if, when removing an electron, all the other electrons did not

hν = 1486.6eV

K.E._{1s}

K.E. (Auger)

∞ -------- 0
2p —**— ε_{2p}~10eV
2s —**— ε_{2s}~20eV

ε(eV)

**

1s —*—*— ε_{1s}~290eV

—*—0

a

c

No. of electrons

C(1s)

C(2s)

C(2p)

C (Auger)

0   400   800   1200
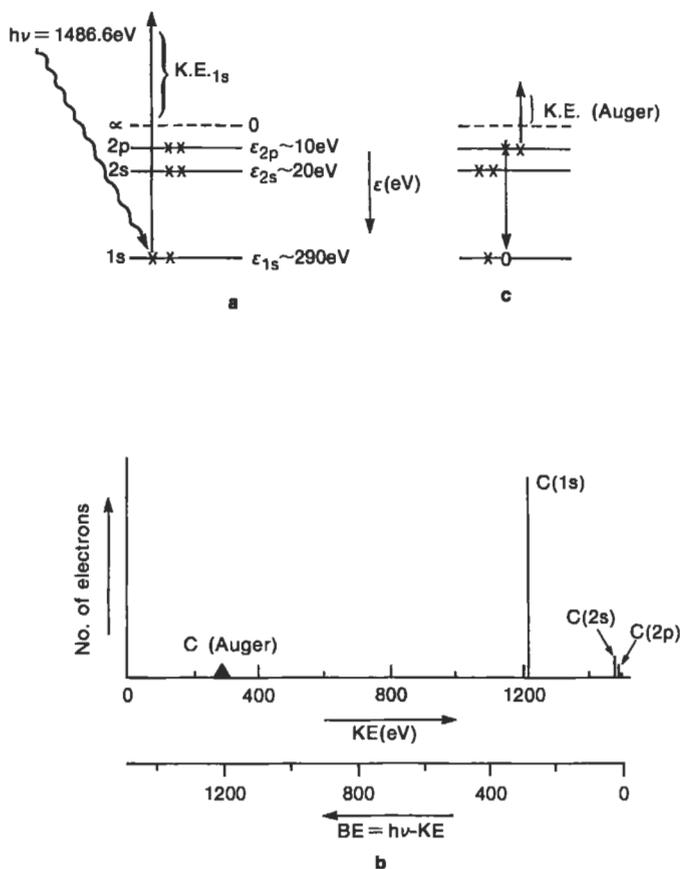
KE(eV)

1200   800   400   0

BE = hν−KE

b

Figure 1 (a) Schematic representation of the electronic energy levels of a C atom and the photoionization of a C 1s electron. (b) Schematic of the *KE* energy distribution of photoelectrons ejected from an ensemble of C atoms subjected to 1486.6-eV X rays.(c) Auger emission relaxation process for the C 1s hole-state produced in (a).

respond in any way). So, by experimentally determining a *BE*, one is approximately determining an ε value, which is specific to the atom concerned, thereby identifying that atom.

Photoelectron Process and Spectrum

Consider what happens if, for example, an ensemble of carbon atoms is subjected to X rays of 1486.6 eV energy (the usual X-ray source in commercial XPS instruments). A carbon atom has 6 electrons, two each in the 1s, 2s, and 2p orbitals, usually written as C $1s^2\,2s^2\,2p^2$. The energy level diagram of Figure 1a represents this electronic structure. The photoelectron process for removing an electron from the

1s level, the most strongly bound level, is schematically shown. Alternatively, for any individual C atom, a 2s or a 2p electron might be removed. In an ensemble of C atoms, all three processes will occur, and three groups of photoelectrons with three different KEs will therefore be produced, as shown in Figure 1b where the KE distribution (the number of ejected photoelectrons versus the kinetic energy)—the photoelectron spectrum—is plotted. Using Equation (1), a BE scale can be substituted for the KE scale, and a direct experimental determination of the electronic energy levels in the carbon atom has been obtained. Notice that the peak intensities in Figure 1b are not identical because the probability for photoejection from each orbital (called the photoionization cross section, σ) is different. The probability also varies for a given orbital (e.g., a 1s orbital) in different atoms and depends on the X-ray energy used. For carbon atoms, using a 1486.6-eV X ray, the cross section for the 1s level, $\sigma_{C\,1s}$ is greater than $\sigma_{C\,2s}$ or $\sigma_{C\,2p}$, and therefore the C 1s XPS peak is largest, as in Figure 1b.

Thus, the number of peaks in the spectrum corresponds to the number of occupied energy levels in the atoms whose BEs are lower than the X-ray energy $h\nu$; the position of the peaks directly measures the BEs of the electrons in the orbitals and identifies the atom concerned; the intensities of the peaks depend on the number of atoms present and on the σ values for the orbital concerned. All these statements depend on the idea that electrons behave independently of each other. This is only an approximation. When the approximation breaks down, additional features can be created in the spectrum, owing to the involvement of some of the passive electrons (those not being photoejected).

Analysis Capabilities

Elemental Analysis

The electron energy levels of an atom can be divided into two types: core levels, which are tightly bound to the nucleus, and valence levels, which are only weakly bound. For the carbon atom of Figure 1, the C 1s level is a core level and the C 2s and 2p levels are valence levels. The valence levels of an atom are the ones that interact with the valence levels of other atoms to form chemical bonds in molecules and compounds. Their character and energy is changed markedly by this process, becoming characteristic of the new species formed. The study of these valence levels is the basis of ultraviolet photoelectron spectroscopy (UPS) discussed in another article in this encyclopedia. The core-level electrons of an atom have energies that are nearly independent of the chemical species in which the atom is bound, since they are not involved in the bonding process. Thus, in nickel carbide, the C 1s BE is within a few eV of its value for elemental carbon, and the Ni 2p BE is within a few eV of its value for Ni metal. The identification of core-level BEs thus provides unique signatures of the elements. All elements in the periodic table can be identified in this manner, except for H and He, which have no core levels. Approximate
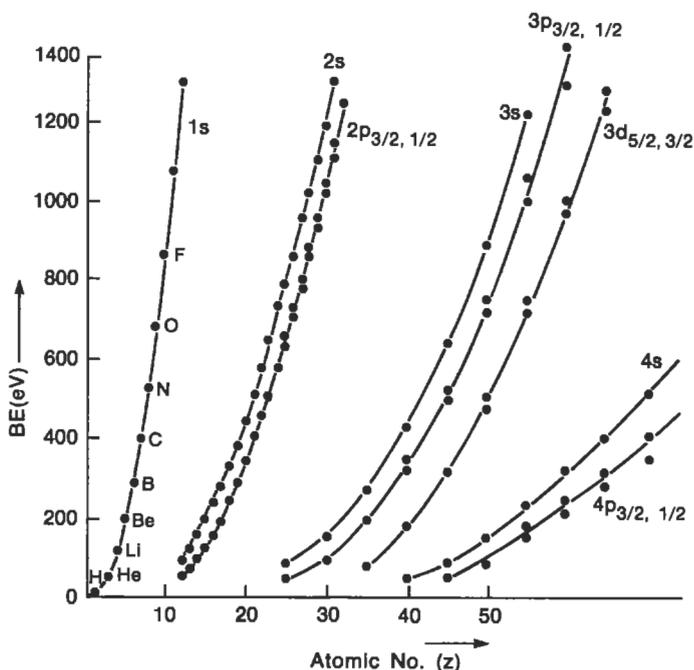
Figure 2   Approximate *BE*s of the different electron shells as a function of atomic number *Z* of the atom concerned, up to the 1486.6-eV limit accessible by Al Kα radiation. [2]

*BE*s of the electrons in all the elements in the period table up to $Z = 70$ are plotted in Figure 2, as a function of their atomic number Z, up to the usual 1486.6-eV accessibility limit.[2] Chance overlaps of *BE* values from core levels of different elements can usually be resolved by looking for other core levels of the element in doubt.

Quantitative analysis, yielding relative atomic concentrations, requires the measurement of relative peak intensities, combined with a knowledge of σ, plus any experimental artifacts that affect intensities. Cross section values are known from well-established calculations,[3] or from experimental measurements of relative peak areas on materials of known composition (standards).[4] A more practical problem is in correctly determining the experimental peak areas owing to variations in peak widths and line shapes, the presence of subsidiary features (often caused by the breakdown of the independent electron model), and the difficulty of correctly subtracting a large background in the case of solids. There are also instrumental effects to account for because electrons of different *KE* are not transmitted with equal efficiency through the electron energy analyzer. This is best dealt with by calibrating the instrument using local standards, i.e., measuring relative peak areas for stan-
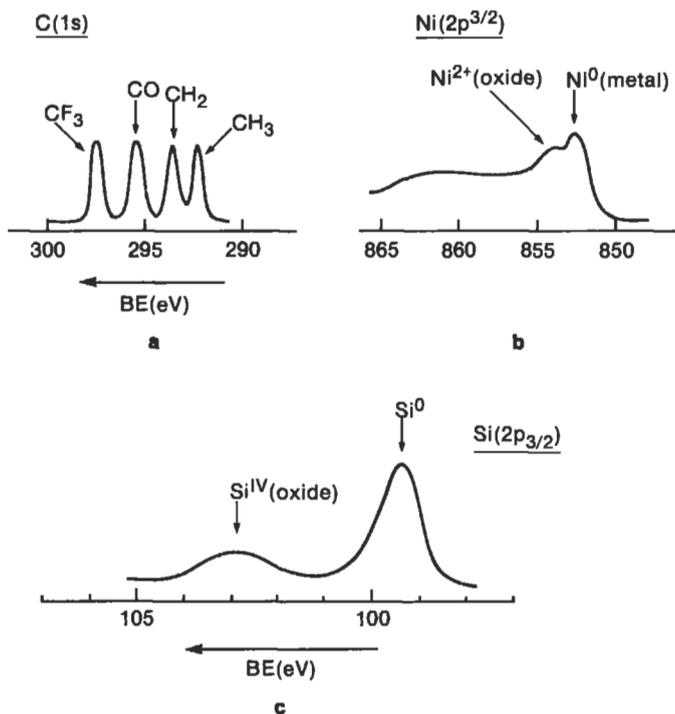
Figure 3　(a) C 1s XPS spectrum from gaseous $CF_3COCH_2CH_3$. (b) Ni $2p_{3/2}$ XPS spectrum from a mixed Ni metal/Ni metal oxide system. (c) Si $2p_{3/2}$ XPS spectrum from a mixed Si/SiO_2 system.

dards of known composition in the same instrument to be used for the samples of unknown composition. Taking all the above into account, the uncertainty in quantification in XPS can vary from a few percent in favorable cases to as high as 30% for others. Practitioners generally know which core levels and which types of materials are the most reliable, and in general, relative differences in composition of closely related samples can be determined with much greater accuracy than absolute compositions.

Chemical State Analysis

Though a core level BE is approximately constant for an atom in different chemical environments, it is not exactly constant. Figure 3a shows the C 1s part of the XPS spectrum of the molecule $CF_3COCH_2CH_3$. Four separated peaks corresponding to the four inequivalent carbon atoms are present.[1] The chemical shift range ΔBE covering the four peaks is about 8 eV compared to the BE of ~290 eV, or ~3%. The carbon atom with the highest positive charge on it, the carbon of the CF_3 group, has the highest BE. This trend of high positive charge and high BE is in accordance

Element	Oxidation state	Chemical shift from zero-valent state
Ni	Ni^{2+}	~2.2 eV
Fe	Fe^{2+}	~3.0 eV
	Fe^{3+}	~4.1 eV
Ti	Ti^{4+}	~6.0 eV
Si	Si^{4+}	~4.0 eV
Al	Al^{3+}	~2.0 eV
Cu	Cu^{+}	~0.0 eV
	Cu^{2+}	~1.5 eV
Zn	Zn^{2+}	~0 eV
W	W^{4+}	2 eV
	W^{6+}	4 eV

Table 1   Typical chemical shift values for XPS core levels.

with the simplest classical electrostatic representation of the atom as a sphere of radius r with a valence charge q on its surface. The potential inside the sphere q/r is felt by the 1s electrons. If q increases, the *BE* of the 1s level increases, and vice versa. This picture is a gross oversimplification because electrons are not so well separated in space, but the general idea that the *BE* increases with increasing charge on the atom holds in the majority of cases. Table 1 lists the approximate chemical shifts found for the different oxidation states of various metals and semiconductors. The typical range is 1 to several eV, though in some important cases (e.g., Cu and Zn) it is very small. Typical spectra illustrating these chemical shifts for a mixed Ni metal/nickel oxide system and a mixed silicon/silicon dioxide system are shown in Figures 3b and 3c.

The spectra of Figure 3 illustrate two further points. All the C 1s peaks in Figure 3a are of equal intensity because there are an equal number of each type of C atom present. So, when comparing relative intensities of the same atomic core level to get composition data, we do not need to consider the photoionization cross section. Therefore, Figure 3c immediately reveals that there is four times as much elemental Si present as SiO_2 in the Si 2p spectrum. The second point is that the chemical shift range is poor compared to the widths of the peaks, especially for the solids in Figures 3b and 3c. Thus, not all chemically inequivalent atoms can be distin-

guished this way. For example, Cu^0 (metal) is not distinguishable from Cu^+ in Cu_2O, and Zn^0 is not distinguishable from Zn^{2+} (e.g., in ZnO).

More Complex Effects

In reality, while the photoelectron is leaving the atom, the other electrons respond to the hole being created. The responses, known as *final state effects*, often lead to additional features in the XPS spectrum, some of which are useful analytically.

An effect that always occurs is a lowering of the total energy of the ion due to the relaxation of the remaining electrons towards the hole. This allows the outgoing photoelectron to carry away greater *KE*, i.e., the *BE* determined is always lower than ε. This needs to be considered when comparing theoretical ε values to experimental *BE*s, i.e., for detailed interpretation of electronic structure effects, but is not generally used analytically.

Spin–orbit splitting results from a coupling of the spin of the unpaired electron left behind in the orbital from which its partner has been photoejected with the angular momentum of that orbital, giving two possible different energy final states (spin up or spin down). It occurs for all levels except s levels, which have no orbital angular momentum (being spherical), turning single peaks into doublet peaks. The splitting increases with Z, as can be seen from Figure 2 in, for example, the $2p_{3/2}$ and $2p_{1/2}$ spin–orbit split components of the 2p level. The only analytical usefulness is that the splitting increases the number of XPS peaks per atom in a completely known way, which can help when overlaps occur.

Some elements, particularly the transition metals, have unpaired electron spins in their valence levels. The degree of unpairing is strongly affected by the bonding process to other atoms. An unpaired core-electron remaining after the photoemission process will couple to any unpaired spin in the valence level, again leading to more than one final state and peak splitting, called multiplet splitting (weaker than the equivalent spin-orbital splitting). Since the degree of unpaired electron spin in the valence levels is strongly affected by chemical bonding, so is the size of the multiplet splitting. For example, the Cr (3s) level of the Cr^{III} ion of Cr_2O_3 is split by 4.2 eV, whereas in the more covalent compound Cr_2S_3 the splitting is 3.2 eV, allowing distinction of Cr^{III} in the two compounds.[5]

While a core-electron is being ejected, there is some probability that a valence electron will be simultaneously excited to an empty orbital level during the relaxation process, Figure 4b. If this shake-up process occurs, the photoelectron must be ejected with less energy, shifting the XPS peak to apparently higher *BE* than for a case where shake-up doesn't occur, as shown in Figure 4c. These "shake-up satellites" in the spectrum are usually weak because the probability of their occurrence is low, but in some cases they can become as strong as the "main" peak. Shake-up structure can provide chemical state identification because the valence levels are involved. A typical example is given in Figure 4d. The ion Cu^{2+} (in CuO) is distin-
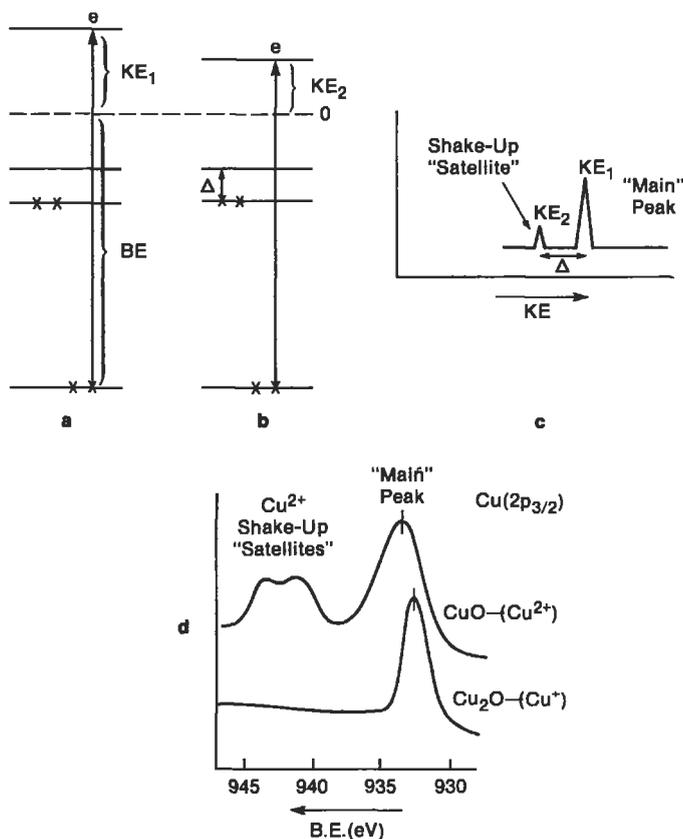
Figure 4 Schematic electron energy level diagram: (a) of a core-level photoelectron ejection process (one electron process); (b) core-level photoelectron ejection process with shake-up (two- electron process); (c) schematic XPS spectrum from (a) plus (b); (d) Cu $2p_{3/2}$ XPS spectrum for Cu^+ in Cu_2O and Cu^{2+} in CuO. The latter shows strong shake-up features.

guishable from Cu^+ (in Cu_2O) by the presence of the very characteristic strong Cu 2p shake-up structure for Cu^{2+}. The chemical shift between Cu^{2+} and Cu^+ could also be used for identification, provided accurate *BE*s are measured. It is sometimes an advantage not to have to rely on accurate *BE*s, for instance, when comparing data of different laboratories or if there is a problem establishing an accurate value because of sample charging. In such cases the "fingerprinting" pattern identification of a main peak plus its satellites, as in Figure 4d, is particularly useful.

After the photoemission process is over, the core-hole left behind can eventually be filled by an electron dropping into it from another orbital, as shown in Figure 1c for the example of carbon. The energy released, in this example $\varepsilon_{1s} - \varepsilon_{2p}$, may be

sufficient to eject another electron. The example of a 2p electron being ejected is shown. This is called Auger electron emission and the approximate KE of the ejected Auger electron will be

$$KE(\text{Auger}) = (\varepsilon_{1s} - \varepsilon_{2p}) - \varepsilon_{2p} \qquad (2)$$

The value is characteristic of the atomic energy levels involved and, therefore, also provides a direct element identification (see the article on AES). The KE (Auger) is independent of the X-ray energy $h\nu$ and therefore it is not necessary to use monochromatic X rays to perform Auger spectroscopy. Therefore, the usual way Auger spectroscopy is performed is to use high- energy electron beams to make the core-holes, as discussed in the AES article. We mention the process here, however, because when doing XPS the allowable Auger process peaks are superimposed on the spectrum, and they can be used as an additional means of element analysis. Also, in many cases, chemical shifts of Auger peaks, which have a similar origin to XPS core-level shifts, are larger, allowing chemical state identification in cases where it is not possible directly from the XPS core levels. For example, Zn^{2+} can be distinguished from Zn^0 by a 3-eV shift in Auger peak KE, whereas it was mentioned earlier that the two species were not distinguishable using XPS core levels.

Surface Sensitivity

Electrons in XPS can travel only short distances through solids before losing energy in collisions with atoms. This inelastic scattering process, shown schematically in Figure 5a, is the reason for the surface sensitivity of XPS. Photoelectrons ejected from atoms "very near" the surface escape unscattered and appear in the XPS peaks. Electrons originating from deeper have correspondingly reduced chances of escaping unscattered and mostly end up in the background at lower KE after the XPS peak, as in Figure 5b. Thus, the peaks come mostly from atoms near the surface, the background mostly from the bulk.

If I_0 is the flux of electrons originating at depth d, the flux emerging without being scattered, I_d, exponentially decreases with depth according to

$$I_d = I_0^{\frac{-d}{\lambda_e \sin\theta}} \qquad (3)$$

where θ is the angle of electron emission and $d/\sin\theta$ is the distance travelled through the solid at that angle. The quantity λ_e is called the *inelastic mean free path length*. The value of λ_e, which determines quantitatively exactly how surface sensitive the measurement is, depends on the KE of the electron and the material through which it travels. Empirical relationships between λ_e and KE are plotted in Figure 6 for elements and for compounds.[6] They are meant as rough guides because values can vary considerably (by a factor of almost 4), depending on what element
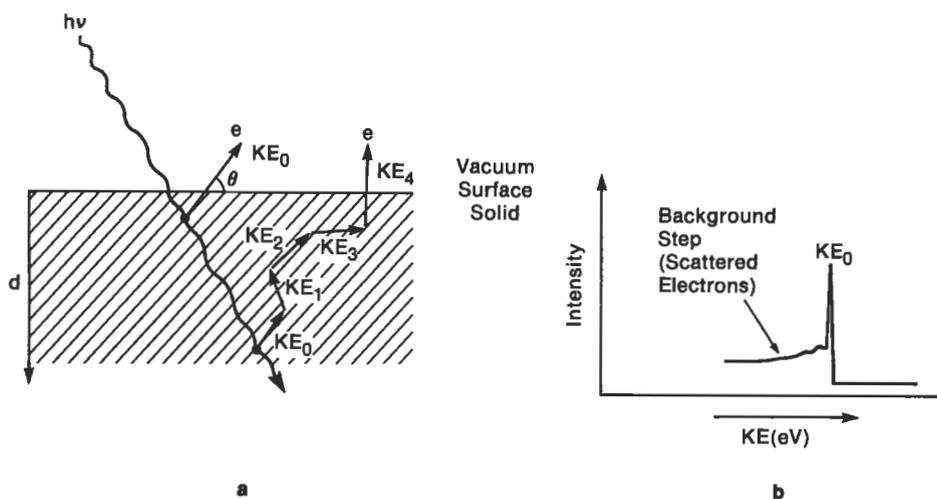
Figure 5 (a) Schematic of inelastic electron scattering occurring as a photoelectron, initial energy KE_0, tries to escape the solid, starting at different depths. $KE_4 < KE_3 < KE_2 < KE_1 < KE_0$. (b) KE energy distribution (i.e., electron spectrum) obtained due to the inelastic scattering in (a). Note that the peak, at E_0, must come mainly from the surface region, and the background step, consisting of the lower energy scattered electrons, from the bulk.

or compound is involved. Substituting λ_e values from the curves into Equation (3) tells us that for normal emission ($\theta = 90°$) using a 200-eV KE XPS peak, 90% of the signal originates from the top ~25 Å, for elements. For a 1400-eV peak the depth is ~60 Å. The numbers are about twice as big for compounds. Thus, the depth probed by XPS varies strongly depending on the XPS peaks used and the material involved. The depth probed can also be made smaller for any given XPS peak and material by detecting at grazing emission angle θ. For smooth surfaces, values down to 10° are practical, for which the depth probed is reduced by a factor of 1/sin 10, or ~6, compared to 90°, from Equation (3). Varying KE or θ are important practical ways of distinguishing what is in the outermost atomic layers from what is underneath.

Instrumentation

An XPS spectrometer schematic is shown in Figure 7. The X-ray source is usually an Al- or Mg-coated anode struck by electrons from a high voltage (10–15 kV) Alkα or Mgkα radiation lines produced at energies of 1486.6 eV and 1256.6 eV, with line widths of about 1 eV. The X rays flood a large area (~1 cm²). The beam's spot size can be improved to about 100-μm diameter by focusing the electron beam
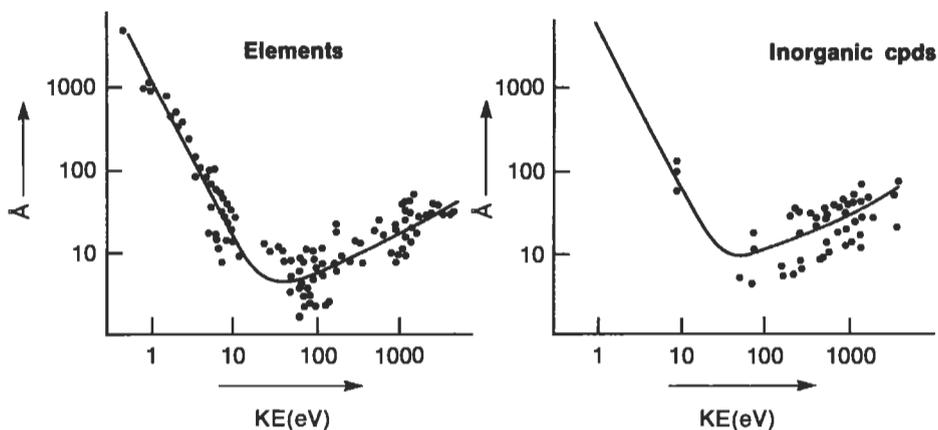
Figure 6   **Mean free path lengths λ_e as a function of *KE*, determined for (a) metals and (b) inorganic compounds.**[6]

onto the anode and passing the X rays through an X-ray monochromator. The latter also improves line widths to between 0.5 and 0.25 eV, leading to higher resolution spectra (thus improving the chemical state identification process) and removing an unwanted X-ray background at lower energies.

Practical limits to the shape and size of samples are set by commercial equipment design. Some will take only small samples (e.g., 1 cm × 1 cm) while others can handle whole 8-in computer disks. Flat samples improve signal strength and allow quantitative θ variation, but rough samples and powders are also routinely handled. Insulating samples may charge under the X-ray beam, resulting in inaccurate *BE* determinations or spectra distorted beyond use. The problem can usually be mitigated by use of a low-energy electron flood gun to neutralize the charge, provided this does not damage the sample.

The electron lenses slow the electrons before entering the analyzer, improving energy resolution. They are also used to define an analyzed area on the sample from which electrons are received into the analyzer and, in one commercial design, to image the sample through the analyzer with 10-μm resolution. Older instruments may have slits instead of lenses. The most popular analyzer is the hemispherical sector, which consists of two concentric hemispheres with a voltage applied between them. This type of analyzer is naturally suited to varying θ by rotating the sample, Figure 7. The XPS spectrum is produced by varying the voltages on the lenses and the analyzer so that the trajectories of electrons ejected from the sample at different energies are brought, in turn, to a focus at the analyzer exit slit. A channeltron type electron multiplier behind the exit slit of the analyzer amplifiers individual electrons by 10^5–10^6, and each such pulse is fed to external conventional pulse counting electronics and on into a computer. The computer also controls the lens and
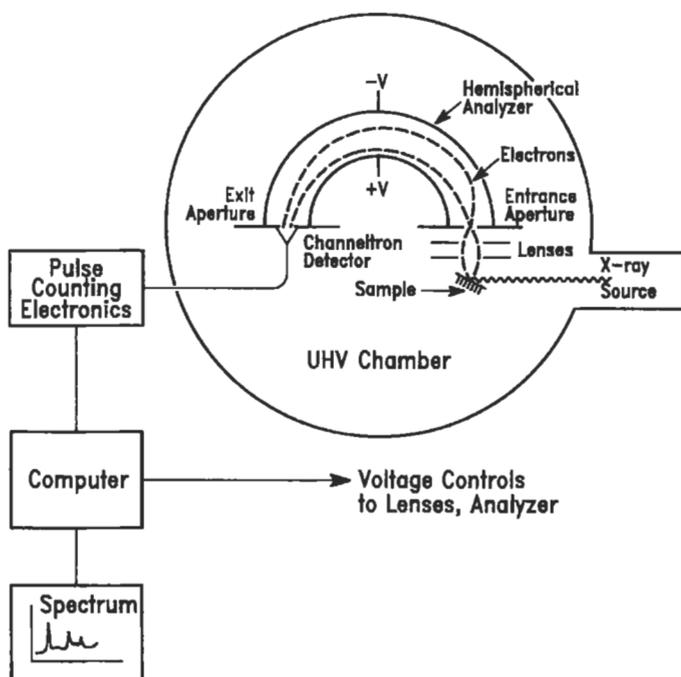
−V

Hemispherical
Analyzer

Electrons

Exit
Aperture

+V

Entrance
Aperture

Pulse
Counting
Electronics

Channeltron
Detector

Lenses

Sample

X−ray
Source

UHV Chamber

Computer

Voltage Controls
to Lenses, Analyzer

Spectrum

Figure 7   **Schematic of a typical electron spectrometer showing all the necessary components. A hemispherical electrostatic electron energy analyser is depicted.**

analyzer voltages. A plot of electron pulses counted against analyzer–lens voltage gives the photoelectron spectrum. More sophisticated detection schemes replace the exit slit–multiplier arrangement with a multichannel array detector. This is the modern equivalent of a photographic plate, allowing simultaneous detection of a range of *KE*s, thereby speeding up the detection procedure.

Commercial spectrometers are usually bakeable, can reach ultrahigh-vacuum pressures of better than 10^{-9} Torr, and have fast-entry load-lock systems for inserting samples. The reason for the ultrahigh-vacuum design, which increases cost considerably, is that reactive surfaces, e.g., clean metals, contaminate rapidly in poor vacuum (1 atomic layer in 1 s at 10^{-6} Torr). If the purpose of the spectrometer is to always look at as-inserted samples, which are already contaminated, or to examine rather unreactive surfaces (e.g., polymers) vacuum conditions can be relaxed considerably.

Applications

XPS is routinely used in industry and research whenever elemental or chemical state analysis is needed at surfaces and interfaces and the spatial resolution requirements are not demanding (greater than 150 μm). If the analysis is related specifically to the top 10 or so atomic layers of air-exposed sample, the sample is simply inserted and data taken. Examples where this might be appropriate include: examination for and identification of surface contaminants; evaluation of materials processing steps, such as cleaning procedures, plasma etching, thermal oxidation, silicide thin-film formation; evaluation of thin-film coatings or lubricants (thickness–quantity, chemical composition); failure analysis for adhesion between components, air oxidation, corrosion, or other environmental degradation problems, tribological (wear) activity; effectiveness of surface treatments of polymers and plastics; surface composition differences for alloys; examination of catalyst surfaces before and after use, after "activation" procedures, and unexplained failures.

Figure 3c was used to illustrate that Si^{IV} could be distinguished from Si^0 by the Si 2p chemical shift. The spectrum is actually appropriate for an oxidized Si wafer having an ~10-Å SiO_2 overlayer. That the SiO_2 is an overlayer can easily be proved by decreasing θ to increase the surface sensitivity; the Si^0 signal will decrease relative to the Si^{IV} signal. The 10-Å thickness can be determined from the Si^{IV}/Si^0 ratio and Equation (3), using the appropriate λ_e value. That the overlayer is SiO_2 and not some other Si^{IV} compound is easily verified by observing the correct position (*BE*) and intensity of the O 1s peak plus the absence of other element peaks. If the sample has been exposed to moisture, including laboratory air, the outermost atomic layer will actually be hydroxide, not oxide. This is easily recognized since there is a chemical shift between OH and O in the O 1s peak position.

Figure 8 shows a typical example where surface modification to a polymer can be followed.[7] High-density polyethylene $(CH_2CH_2)_n$ was surface-fluorinated in a dilute fluorine–nitrogen mixture. Spectrum A was obtained after only 0.5 s treatment. A F 1s signal corresponding to about a monolayer has appeared, and CF formation is obvious from the chemically shifted shoulder on the C 1s peak at the standard CF position. After 30 s reaction, the F 1s / C 1s ratio indicates (spectrum B) that the reaction has proceeded to about 30 Å depth, and that CF_2 formation has occurred, judging by the appearance of the C 1s peak at 291 eV. Angular studies and more detailed line shape and relative intensity analysis, compared to standards, showed that for the 0.5-s case, the top monolayer is mainly polyvinyl fluoride $(CFHCH_2)_n$, whereas after 30 s polytrifluoroethylene $(CF_2CFH)_n$ dominates in the top two layers. While this is a rather aggressive example of surface treatment of polymers, similar types of modifications frequently are studied using XPS. An equivalent example in the semiconductor area would be the etching processes of Si/SiO_2 in CF_4/O_2 mixtures, where varying the CF_4/O_2 ratio changes the relative etching rates of Si and SiO_2, and also produces different and varying amounts of residues at the wafer's surface.
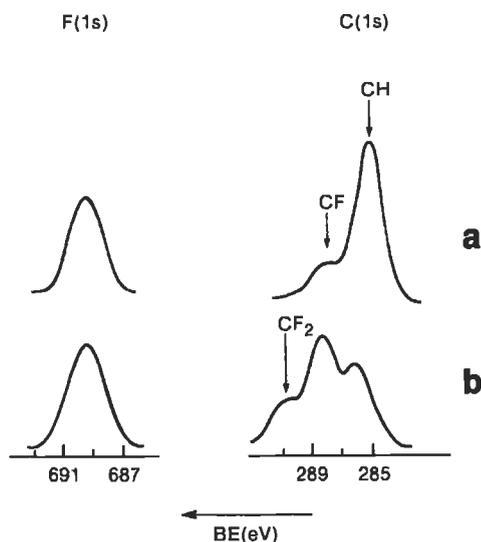
F(1s)   C(1s)

Figure 8   XPS spectrum in the C 1s and F 1s regions of polyethylene $(CH_2)_n$, treated with a dilute F_2/N_2 gaseous mixture for (a) 0.5 sec, and (b) 30 sec.[7]

In many applications the problem or property concerned is not related just to the top 10 or so atomic layers. Information from deeper regions is required for a number of reasons: A thick contaminant layer, caused by air exposure, may have covered up the surface of interest; the material may be a layered structure in which the buried interfaces are important; the composition modulation with depth may be important, etc. In such cases, the 2–15 atomic layer depth resolution attainable in XPS by varying θ is insufficient, and some physical means of stripping the surface while taking data, or prior to taking data, is required. This problem is common to all very surface sensitive spectroscopies. The most widely used method is argon ion sputtering, done inside the spectrometer while taking data. It can be used to depths of μm, but is most effective and generally used over much shorter distances (hundreds and thousands of Å) because it can be a slow process and because sputtering introduces artifacts that get worse as the sputtered depth increases.[8] These include interfacial mixing caused by the movement of atoms under the Ar^+ beam, elemental composition alteration caused by preferential sputtering of one element versus another, and chemical changes caused by bonds being broken by the sputtering process.

If the interface or depth of interest is beyond the capability of sputtering, one can try polishing down, sectioning, or chemical etching the sample before insertion.

The effectiveness of this approach varies enormously, depending on the material, as does the extent of the damaged region left at the surface after this preparation treatment.

In some cases, the problem or property of interest can be addressed only by performing experiments inside the spectrometer. For instance, metallic or alloy embrittlement can be studied by fracturing samples in ultrahigh vacuum so that the fractured sample surface, which may reveal why the fracture occurred in that region, can be examined without air exposure. Another example is the simulation of processing steps where exposure to air does not occur, such as many vacuum deposition steps in the semiconductor and thin-film industries. Studying the progressive effects of oxidation on metals or alloys inside the spectrometer is a fairly well-established procedure and even electrochemical cells are now coupled to XPS systems to examine electrode surfaces without air exposure. Sometimes materials being processed can be capped by deposition of inert material in the processing equipment (e.g., Ag, Au, or in GaAs work, arsenic oxide), which is then removed again by sputtering or heating after transfer to the XPS spectrometer. Finally, attempts are sometimes made to use "vacuum transfer suitcases" to avoid air exposure during transfer.

Comparison with other Techniques

XPS, AES, and SIMS are the three dominant surface analysis techniques. XPS and AES are quite similar in depth probed, elemental analysis capabilities, and absolute sensitivity. The main XPS advantages are its more developed chemical state analysis capability, somewhat more accurate elemental analysis, and far fewer problems with induced sample damage and charging effects for insulators. AES has the advantage of much higher spatial resolutions (hundreds of Å compared to tens of μm), and speed. Neither is good at trace analysis, which is one of the strengths of SIMS (and related techniques). SIMS also detects H, which neither AES nor XPS do, and probes even less deeply at the surface, but is an intrinsically destructive technique. Spatial resolution is intermediate between AES and XPS. ISS is the fourth spectroscopy generally considered in the "true surface analysis" category. It is much less used, partly owing to lack of commercial instrumentation, but mainly because it is limited to elemental analysis with rather poor spectral distinction between some elements. It is, however, the most surface sensitive elemental analysis technique, seeing only the top atomic layer. With the exception of EELS and HREELS, all other spectroscopies used for surface analysis are much less surface sensitive than the above four. HREELS is a vibrational technique supplying chemical functional group information, not elemental analysis, and EELS is a rarely used and specialized technique, which, however, can detect hydrogen.

Conclusions

XPS has developed into the most generally used of the truly surface sensitive techniques, being applied now routinely for elemental and chemical state analysis over a range of materials in a wide variety of technological and chemical industries. Its main current limitations are the lack of high spatial resolutions and relatively poor absolute sensitivity (i.e., it is not a trace element analysis technique). Recently introduced advances in commercial equipment have improved speed and sensitivity by using rotating anode X-ray sources (more photons) and parallel detection schemes. Spot sizes have been reduced from about 150 μm, where they have languished for several years, to 75 μm. Spot sizes of 10 μm have been achieved, and recently anounced commercial instruments offer these capabilities. When used in conjunction with focused synchrotron radiation in various "photoelectron microscope" modes higher resolution is obtainable. Routinely available 1 μm XPS resolution in laboratory-based equipment would be a major breakthrough, and should be expected within the next three years.

Special, fully automated one-task XPS instruments are beginning to appear and will find their way into both quality control laboratories and process control on production lines before long.

More detailed discussions of XPS can be found in references 4–12, which encompass some of the major reference texts in this area.

Related Articles in the Encyclopedia

UPS, AES, SIMS, and ISS

References

1   K. Siegbahn et al. *ESCA: Atomic, Molecular, and Solid State Structure Studied by Means of Electron Spectroscopy.* Nova Acta Regime Soc. Sci., Upsaliensis, 1967, Series IV, Volume 20; and K. Siegbahn et al. *ESCA Applied to Free Molecules.* North Holland, Amsterdam, 1969. These two volumes, which cover the pioneering work of K.Siegbahn and coworkers in developing and applying XPS, are primarily concerned with chemical structure identification of molecular materials and do not specifically address surface analysis.

2   Charts such as this, but in more detail, are provided by all the XPS instrument manufacturers. They are based on extensive collections of data, much of which comes from Reference 1.

3   J. H. Scofield. *J. Electron Spect.* **8,** 129, 1976. This is the standard quoted reference for photoionization cross sections at 1487 eV. It is actually one of the most heavily cited references in physical science. The calculations are published in tabular form for all electron level of all elements.

See, for example, S. Evans et al. *J. Electr. Spectr.* **14,** 341, 1978. Relative experimental ratios of cross sections for the most intense peaks of most elements are given.

5 J. C. Carver, G. K. Schweitzer, and T. A. Carlson. *J. Chem. Phys.* **57,** 973, 1972. This paper deals with multiplet splitting effects, and their use in distinguishing different element states, in transition metal complexes.

6 M. P. Seah and W. A. Dench. *Surf. Interface Anal.* **1,** 1, 1979. Of the many compilations of measured mean free path length versus *KE,* this is the most thorough, readable, and useful.

7 D. T. Clark, W. J. Feast, W. K. R. Musgrave, and I. Ritchie. *J. Polym. Sci. Polym. Chem.* **13,** 857, 1975. One of many papers from Clark's group of this era which deal with all aspects of XPS of polymers.

8 See the article on surface roughness in Chapter 12.

9 The book series *Electron Spectroscopy: Theory, Techniques, and Applications,* edited by C. R. Brundle and A. D. Baker, published by Academic Press has a number of chapters in its 5 volumes which are useful for those wanting to learn about the analytical use of XPS: In Volume 1, *An Introduction to Electron Spectroscopy* (Baker and Brundle); in Volume 2, *Basic Concepts of XPS* (Fadley); in Volume 3, *Analytical Applications of XPS* (Briggs); and in Volume 4, *XPS for the Investigation of Polymeric Materials* (Dilks).

10 T. A. Carlson, *Photoelectron and Auger Spectroscopy,* Plenum, 1975. A complete and largely readable treatment of both subjects.

11 *Practical Surface Analysis,* edited by D. Briggs and M. P. Seah, published by J. Wiley; *Handbook of XPS and UPS,* edited by D. Briggs. Both contain extensive discussion on use of XPS for surface and material analysis.

12 *Handbook of XPS,* C. D. Wagner, published by PHI (Perkin Elmer). This is a book of XPS data, invaluable as a standard reference source.

5.2   UPS

Ultraviolet Photoelectron Spectroscopy

C. R. BRUNDLE

Contents

- Introduction
- Basic Principles
- Analysis Capabilities
- Conclusions

Introduction

The photoelectric process, which was discovered in the early 1900s, was developed as a means of studying the electronic structure of molecules in the gas phase in the early 1960s, largely owing to the pioneering work of D. W. Turner's group.[1] A major step was the introduction of the He resonance discharge lamp as a laboratory photon source, which provides monochromatic 21.2-eV light. In conjunction with the introduction of high resolution electron energy analyzers, this enables the binding energies (BE) of all the electron energy levels below 21.2 eV to be accurately determined with sufficient spectral resolution to resolve even vibrational excitations. Coupled with theoretical calculations, these measurements provide information on the bonding characteristics of the valence-level electrons that hold molecules together. The area has become known as ultraviolet photoelectron spectroscopy (UPS) because the photon energies used (21.2 eV and lower) are in the vacuum ultraviolet (UV) part of the light spectrum. It is also known as molecular photoelectron spectroscopy, because of its ability to provide molecular bonding information.

In parallel with these developments for studying molecules, the same technique was being developed independently to study solids; particularly metals and semi-

conductors.[2] This branch of the technique is usually known as UV photoemission. Here the electronic structure of the solid (the band structure for metals and semi-conductors) was the interest. Since the technique is sensitive to only the top few atomic layers, the electronic structure of the surface, which in general can be different from that of the bulk, is actually obtained. The two branches of UPS, gas-phase and solid-surface studies, come together when adsorption and reaction of molecules at surfaces is studied.[3, 4]

Though commercial UPS instruments were sold in the 1970s, for gas-phase work, none are sold today. Since the only additional item required to perform UPS on an XPS instrument is a He source, this is usually how UPS is performed in the laboratory. An alternative, more specialized approach, is to couple an electron spectrometer to the beam-line monochromator of a synchrotron facility. This provides a tunable source of light, usually between around 10 eV and 200 eV, though many beam lines can obtain much higher energies. This approach can provide a number of advantages, including variable surface sensitivity and access to core levels up to the photon energy used, at much higher resolution than obtainable by laboratory XPS instruments. Even using a laboratory UPS source, such as a He resonance lamp, some low-lying core levels are accessible. When using either synchrotron or laboratory sources to access core levels, all the materials surface analysis capabilities of XPS described in the preceding article become available.

Basic Principles

The photoionization process and the way it is used to measure BEs of electrons to atoms is described in the article on XPS and will not be repeated here. Instead, we will concentrate on the differences between the characteristics of core-level BEs, described in the XPS article, and those of valence-level BEs. In Figure 1a the electron energy-level diagram for a CO molecule is shown, schematically illustrating how the atomic levels of the C and O atom interact to form the CO molecule. The important point to note is that whereas the BEs of the C 1s and O 1s core levels remain characteristic of the atoms when the CO molecule is formed (the basis of the use of XPS as an elemental analysis tool), the C 2p and O 2p valence levels are no longer characteristic of the individual atoms, but have combined to form a new set of molecular orbitals entirely characteristic of the CO molecule. Therefore, the UPS valence-band spectrum of the CO molecule, Figure 1b, is also entirely characteristic of the molecule, the individual presence of a C atom and an O atom no longer being recognizable. For a solid, such as metallic Ni, the valence-level electrons are smeared out into a band, as can be seen in the UPS spectrum of Ni (Figure 2a). For molecules adsorbed on surfaces there is also a smearing out of structure. For example, Figure 2b shows a monolayer of CO adsorbed on an Ni surface.
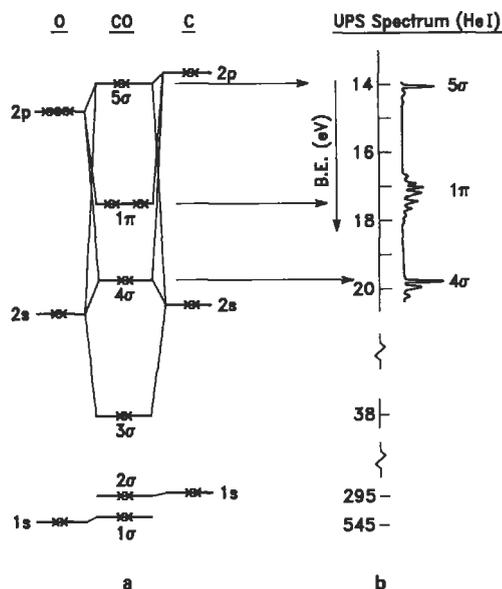
Figure 1 (a) Electron energy diagram for the CO molecule, illustrating how the molecular orbitals are constructed from the atomic levels. (b) He I UPS spectrum of CO.[1]

Analytical Capabilities

As stated earlier, the major use of UPS is not for materials analysis purposes but for electronic structure studies. There are analysis capabilities, however. We will consider these in two parts: those involving the electron valence energy levels and those involving low-lying core levels accessible to UPS photon energies (including synchrotron sources). Then we will answer the question "why use UPS if XPS is available?"

Valence Levels

The spectrum of Figure 1b is a fingerprint of the presence of a CO molecule, since it is different in detail from that of any other molecule. UPS can therefore be used to identify molecules, either in the gas phase or present at surfaces, provided a data bank of molecular spectra is available, and provided that the spectral features are sufficiently well resolved to distinguish between molecules. By now the gas phase spectra of most molecules have been recorded and can be found in the literature.[1, 5] Since one is using a pattern of peaks spread over only a few eV for identification purposes, mixtures of molecules present will produce overlapping patterns. How well mixtures can be analyzed depends, obviously, on how well overlapping peaks can be resolved. For molecules with well-resolved fine structure (vibrational) in the spectra (see Figure 1b), this can be done much more successfully than for the broad,
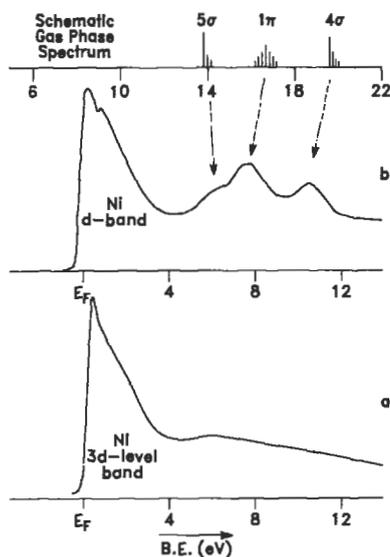
Schematic Gas Phase Spectrum

5σ 1π 4σ

6   10   14   18   22

Ni d–band

E_F 4 8 12

b

Ni 3d–level band

E_F 4 8 12

a

B.E. (eV)

Figure 2 (a) He II UPS spectrum of a Ni surface.[4] (b) He II UPS spectrum of a CO mono-layer adsorbed on a Ni surface.[4] Note the broadening and relative binding-energy changes of the CO levels compared to the gas phase spectrum. Gas-phase binding energies were measured with respect to the vacuum level; solid state binding energies relative to the Fermi level E_F.

unresolved bands found for solid surfaces (see Figure 2b). For solids that have electronic structure characteristics in between those of molecules and metals, such as polymers, ionic compounds, or molecules adsorbed on surfaces (Figure 2b), enough of the individual molecular-like structure of the spectra often remains for the valence levels to be used for fingerprinting purposes. Reactions between molecules and surfaces often can be fingerprinted also. For example, in Figure 3 the UPS differences between molecular H_2O on a metal, and its only possible dissociation fragments, OH and atomic O, are schematically illustrated.

The examples of valence-level spectra given so far, for solid surfaces, i.e., those in Figures 2a, 2b, and 3, are all *angle-integrated* spectra; that is, electrons emitted over a wide solid angle of emission are collected and displayed. In fact, the energy distribution of photoemitted electrons from solids varies somewhat depending on the direction of emission and if data is taken in an angular-resolved mode, that is, for specific directions for the photon beam and the photoemitted electrons, detailed information about the three-dimensional (3D) band structure of the solid, or the two-dimensional (2D) band structure of an adsorbate overlayer may be obtained, together with information on the geometric orientation of such adsorbate mole-
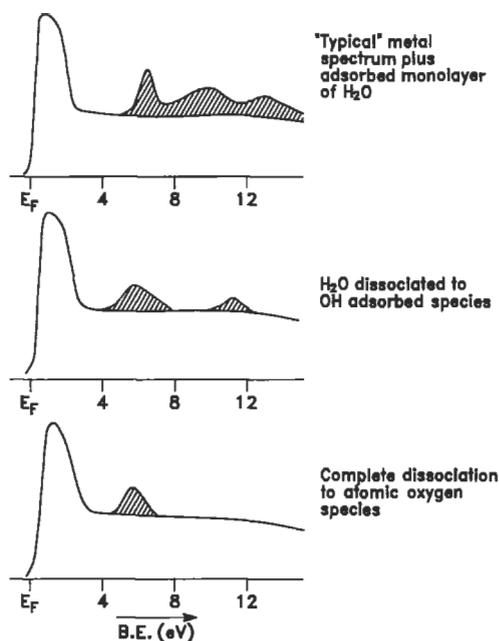
Figure 3 Schematic spectra of H_2O, OH, and atomic O adsorbed on a metal surface illustrate how molecules can be distinguished from their reactor products by fingerprinting.

cules. To properly exploit the technique requires also variation of the photon energy, $h\nu$ (therefore requiring synchrotron radiation) and the polarization of the radiation (s and p, naturally available from the synchrotron source). Basically, recording the UPS spectrum while varying all these parameters (angle, photon energy, and polarization) picks out specific parts of the density of states. A fuller description of this type of work[6] is beyond the scope of this article and is not particularly relevant to materials analysis, except for the fact that molecular orientation at surfaces can be determined. This property is, however, restricted to situations with long-range order, i.e., 2D arrays of molecules on single-crystal surfaces.

Low-Lying Accessible Core Levels

Table 1 lists core levels and their BEs for elements commonly used in technology, which are sufficiently sharp and intense, and which are accessible to laboratory He I or He II sources (21.2-eV or 40.8-eV photon energy) or to synchrotron sources (up to 200 eV or higher). The analytical approaches are the same as described in the XPS article. For example, in that article examples were given of Si 2p spectra obtained using a laboratory Al Kα X-ray source at 1486-eV photon energy. The

Element	Core level	Approximate binding energy (eV)	Usable r radiation
Al	2p	72	S
Si	2p	100	S
S	2p	164	S
Zn	3d	9	He I, He II, S
Ga	3d	18	He I, He II, S
Ge	3d	29	He II, S
As	3d	41	S
Ta	4f	25	He II, S
W	4f	34	S
Ir	4f	60	S
Pt	4f	70	S
Au	4f	84	S
Hg	4f	99	S
	5d	7	He I, He II, S
Pb	4f	138	S

Table 1 Narrow, intense core levels of some elements commonly used in technological materials that are accessible to He I / He II radiation, or synchrotron radiation below 200 eV.

Si 2p line, at about 100 eV BE, is also easily accessible at most synchrotron sources but cannot, of course, be observed using He I and He II radiation. On the other hand, the Zn 3d and Hg 4f lines can be observed quite readily by He I radiation (see Table 1) and the elements identified in this way. Quantitative analysis using relative peak intensities is performed exactly as in XPS, but the photoionization cross sections σ are very different at UPS photon energies, compared to Al Kα energies, and tabulated or calculated values are not so readily available. Quantitation, therefore, usually has to be done using local standards.
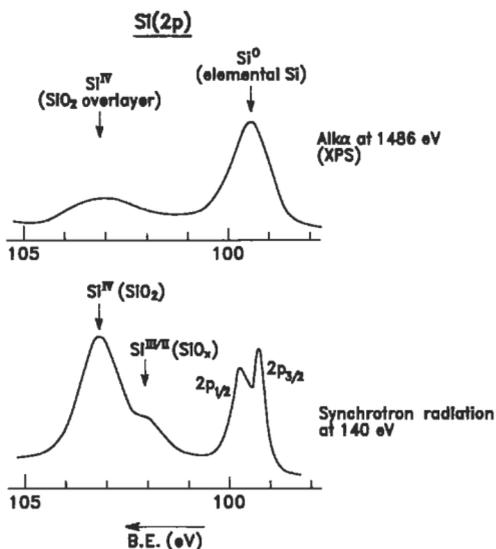
Si(2p)

Figure 4   Schematic comparison of the Si 2p spectra of an Si/SiO₂ interface taken using Al K radiation at 1486 eV and synchrotron radiation at 40 eV photon energy. Note the greater surface sensitivity and higher resolution in the synchrotron case.

Why Use UPS for Analysis?

Since all the valence levels and core levels that are accessible to UPS photon sources are also accessible to XPS, what are the reasons for ever wanting to use laboratory He sources or synchrotron radiation? There are at least four significant differences that can be important analytically in special circumstances. First, the surface sensitivity is usually greater in UPS because for a given energy level being examined, the lower photon energy sources in UPS yield ejected photoelectrons having lower kinetic energies. For example, the Si 2p signal of Figure 3 in the XPS article consists of electrons having a kinetic energy 1486–100 eV = 1386 eV. If the Si 2p spectrum were recorded using 140 eV synchrotron photons, the kinetic energy would be 140–100 eV = 40 eV. Looking at the inelastic mean-free path length diagram of Figure 6 in the XPS article, one can see that 40-eV photoelectrons have about one-third the inelastic scattering length of 1400-eV electrons. Therefore the synchrotron recorded signal would be roughly three times as surface sensitive, as illustrated in Figure 4 where the XPS SiO₂ / Si spectrum is schematically compared for 1486 eV and 140 eV photon sources. The SiO₂ part of the Si 2p signal is much stronger in the synchrotron spectrum and therefore much thinner layers will be more easily detectable.

Secondly, spectral resolution can be significantly higher for UPS or synchrotron data, compared to XPS. This is simply a consequence of UPS (synchrotron) sources

having narrower line widths than laboratory X-ray sources. Thus, whereas the XPS recorded Si 2p signal of Figure 4 has a width of about 1 eV, the individual $2p_{3/2}$ and $2p_{1/2}$ components of the synchrotron recorded signal are only about 0.25 eV wide. Whether this resolution improvement can be achieved in any individual case depends on the natural line width of the particular core level concerned. Si 2p, W 4f, Al 2p, Pt 4f, and Au 4f are all examples of narrow core lines, where a large resolution improvement would occur using synchrotron sources, allowing small chemical shifts corresponding to chemically distinct species to be more easily seen. For valence levels, higher resolution is also an obvious advantage since, as described earlier, one is usually looking at several lines or bands, which may overlap significantly. Two additional practical points about resolution also should be noted. The spectral resolution of the gratings used to monochromatize synchrotron radiation gets worse as the photon energy gets higher, so the resolution advantage of synchrotron radiation decreases as one goes to high BE core levels. Second, monochromators can be used with laboratory X-ray sources, improving XPS resolution significantly, but not to the degree achievable in UPS or synchrotron work.

The third significant difference between UPS and XPS, from an analytical capability point of view, concerns signal strength. To zeroth order, σ values are a maximum for photon energies just above photoionization threshold, and then decrease strongly as the photon energy is increased, so valence levels in particular have much greater σ values using UPS or synchrotron sources, compared to XPS. When coupled with the high photon fluxes available from such sources, this results in greater absolute sensitivity for UPS or synchrotron spectra.

Taking these differences together, one can see that all three work in favor of UPS or synchrotron compared to XPS when trying to observe very thin layers of chemically distinct material at the surface of a bulk material: improved surface sensitivity; improved resolution allowing small surface chemically shifted components in a spectrum to be distinguished from the underlying bulk signal; and improved absolute sensitivity. As a practical matter, one has to ask whether the core levels one wants to use are even accessible to UPS or synchrotron and whether the need to go to a national facility on a very access-limited basis can compare to day-in, day-out laboratory operations. For UPS using He I and He II radiation sources the addition of these to existing XPS system is not excessively costly and is then always there to provide additional capability useful for specific materials and problems.

The final difference between UPS or synchrotron capabilities and XPS, from an analytical point of view, is in lateral resolution. Modern laboratory XPS small-spot instruments can look at areas down to 30–150 μm, depending on the particular instrument, with one very specialized instrument offering imaging capabilities at 10-μm resolution, but with degraded spectroscopy capabilities.[8] For UPS and synchrotron radiation, much higher spatial resolution can be achieved, partly because the lower kinetic energy of the photoelectron lends itself better to imaging schemes and partly because of efforts to focus synchrotron radiation to small spot sizes. The

potential for a true photoelectron microscope with sub 1000-Å resolution therefore exists, but it has not been realized in any practical sense yet.

Conclusions

UPS, if defined as the use of He I, He II, or other laboratory low-energy radiation sources (<50 eV), has rather limited materials surface analysis capabilities. Valence and core electron energy levels below the energy of the radiation source used can be accessed and the main materials analysis role is in providing higher resolution and high surface sensitivity data as a supplement to XPS data, usually for the purpose of learning more about the chemical bonding state at a surface. Angle-resolved UPS can supply molecular orientation geometric information for ordered structures on single crystal surfaces, but its main use is to provide detailed band structure information.

Synchrotron radiation can be used to provide the same information, but also has the great advantage of a wider, tunable, photon energy range. This allows one to access some core levels at higher resolution and surface sensitivity than can be done by XPS. The variable energy source also allows one to vary the surface sensitivity by varying the kinetic energy of the ejected photoelectrons, thereby creating a depth profiling capability. Most synchrotron photoemission work to date has involved fundamental studies of solid state physics and chemistry, rather than materials analysis, albeit on such technologically important materials as Si, GaAs, and CdTeHg. Some quite applied work has been done related to the processing of these materials, such as studying the effects of cleaning procedures on residual surface contaminants, and studying reactive ion-etching mechanisms.[9] The major drawback of synchrotron radiation is that it is largely unavailable to the analytical community and is an unreliable photon source for those who do have access. As the number of synchrotron facilities increase and as they become more the domain of people wanting to use them as dedicated light sources, rather than in high-energy physics collision experiments, the situation for materials analysis will improve and the advantages over laboratory-based XPS will be more exploitable. Synchrotron radiation will never replace laboratory-based XPS, however, and it should be regarded as complementary, with advantages to be exploited when really needed. High spatial resolution photoelectron microscopy is likely to become one such area.

Related Articles in the Encyclopedia
XPS and SEXAFS

References

1   D. W. Turner, C. Baker, A. D. Baker, and C. R. Brundle. *Molecular Photoelectron Spectroscopy.* Wiley, London, 1970. This volume presents a brief

introduction to the principles of UPS and a large collection of spectra on small molecules, together with their interpretation in terms of the electronic structure and bonding of the molecules.

2 W. E. Spicer. In *Survey of Phenomena in Ionized Gases.* International Atomic Energy Agency, Vienna, 1968, p. 271. A review of the early photoemission work on solids by the pioneering group in this area.

3 D. Menzel. *J. Vac. Sci. Tech.* **12,** 313, 1975. A review of the applications of UPS to the adsorption of molecules at metal surfaces.

4 C. R. Brundle. In *Molecular Spectroscopy.* (A. R. West, Ed.) Heyden, London, 1976. This review discusses both the use of XPS and UPS in studying adsorption and reactions at surfaces.

5 K. Kimura, S. Katsumata, Y. Achita, Y. Yamazaki, and S. Iwata. *Handbook of He I Photoelectron Spectra of Fundamental Organic Molecules.* Halsted Press, New York, 1981. This volume collects together spectra and interpretation for 200 organic molecules.

6 *Photoemission in Solids.* (L. Ley and M. Cardona, Eds.) Springer-Verlag, New York, 1978 and 1979, Vols. 1 and 2.

7 N. V. Smith and F. J. Himpsel. In *Handbook on Synchrotron Radiation.* (E. E. Koch, Ed.) North Holland, New York, 1983, Vol. 1b.

8 P. Coxon, J. Krizek, M. Humpherson, and I. R. M. Wardell. *J. Elec. Spec.* 821, 1990.

9 J. A. Yarmoff and F. R. McFeely, *Surface Science* 184, 389, 1987.

5.3 AES

Auger Electron Spectroscopy

Y.E. STRAUSSER

Contents

- Introduction
- Basic Principles of Auger
- Information in Auger Spectra
- Methods for Surface and Thin-Film Characterization
- Artifacts That Require Caution
- Conclusions

Introduction

Auger electron spectroscopy (AES) is a technique used to identify the elemental composition, and in many cases, the chemical bonding of the atoms in the surface region of solid samples. It can be combined with ion-beam sputtering to remove material from the surface and to continue to monitor the composition and chemistry of the remaining surface as this surface moves into the sample. It uses an electron beam as a probe of the sample surface and its output is the energy distribution of the secondary electrons released by the probe beam from the sample, although only the Auger electron component of the secondaries is used in the analysis.

Auger electron spectroscopy is the most frequently used surface, thin-film, or interface compositional analysis technique. This is because of its very versatile combination of attributes. It has surface specificity—a sampling depth that varies

between 5 and 100 Å depending upon the energy of the Auger electrons measured and the signal-to-noise ratio in the spectrum. It has good lateral spatial resolution, which can be as low as 300 Å, depending on the electron gun used and the sample material. It has very good depth resolution, as low as 20 Å depending on the characteristics of the ion beam used for sputtering. It has a good absolute detectability, as low as 100 ppm for most elements under good conditions. It can produce a three-dimensional map of the composition and chemistry of a volume of a sample that is tens of μm thick and hundreds of μm on a side.

On the other hand, AES cannot detect H or He. It does not do nondestructive depth profiling. It uses an electron beam as a probe, which can be destructive to some samples. It requires the sample to be put into and to be compatible with high vacuum. Some nonconducting samples charge under electron beam probing and cannot be analyzed. The sputtering process can alter the surface composition and thereby give misleading results. It does turn out to be the technique of choice, in its area, much of the time. The purpose of this article is to make clear what it can and cannot do and how to get the most information from it.

The Auger process, which produces an energetic electron in a radiationless atomic transition, was first described by Pierre Auger in 1923.[1] The detection of Auger electrons in the secondary electron energy spectra produced by electron bombardment of solid samples was reported by J. J. Lander in 1953.[2] Its use in an analytical technique to characterize solid surfaces was made practical by Larry Harris' analog detection circuitry in 1967.[3] From that time the technology developed very rapidly, and the technique gained momentum through the 1970s and 1980s.

As the technique developed so did the instrumentation. The hardware development has taken advantage of improvements in ultrahigh vacuum technology and computerization. Systems are available having 300-Å diameter field emission electron beams; user-friendly, rapidly attained ultrahigh vacuum; and complete computer control of the system. At the other end of the price range are components that can be "plugged in" to various deposition and processing systems to provide *in-situ* surface characterization.

AES, X-Ray Photoelectron Spectroscopy (XPS), Secondary Ion Mass Spectroscopy (SIMS), and Rutherford Backscattering Spectroscopy (RBS) have become the standard set of surface, thin-film, and interface analysis tools. Each has its own strengths, and mostly they are complementary. XPS uses X rays as a probe, which are usually less damaging to the surface than the electron beam of Auger but which can't be focused to give high lateral spatial resolution. XPS is also more often selected to determine chemical information. SIMS can detect H and He and has a much higher absolute sensitivity in many cases, but seldom gives any chemical information and, by its nature, has to remove material to do its analysis. RBS readily produces good quantitative results and does nondestructive depth profiling, but it lacks the absolute sensitivity of Auger to many of the important elements and its depth resolution is not as good as Auger can produce, in many cases.
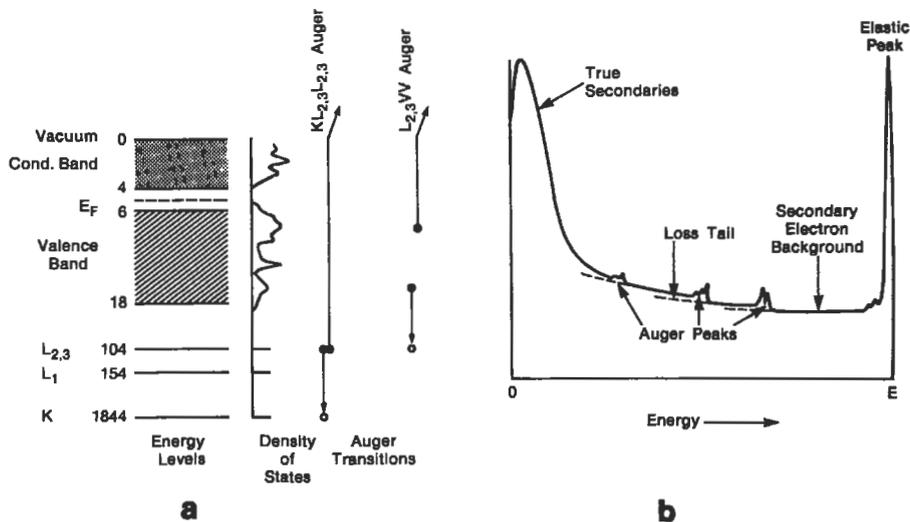
Figure 1 (a) Energy level diagram of solid Si, including the density of states of the valence and conduction bands, a schematic representation of the Si $KL_{2,3}L_{2,3}$ Auger transitions, and a subsequent LVV Auger transition. (b) The complete secondary electron energy distribution produced by the interaction of a primary electron beam of energy E with a solid surface. The true secondary peak, the elastic peak, and some Auger peaks are shown. Also shown are the secondary background and the loss tail contributions to the background from each of the Auger peaks.

Basic Principles of Auger

The basic Auger process involves the production of an atomic inner shell vacancy, usually by electron bombardment, and the decay of the atom from this excited state by an electronic rearrangement and emission of an energetic electron rather than by emission of electromagnetic radiation. For example, as illustrated in Figure 1a, if a Si surface is bombarded by 5-keV electrons, some of the Si atoms will lose electrons from their K shell, whose binding energy is ~1.8 keV. The K shell vacancy will typically be filled by the decay of an electron from one of the L subshells, let's say the $L_{2,3}$ shell, which has a binding energy of 104 eV. This leaves an energy excess of 1.7 keV. This is sometimes relieved by the emission of a 1.7-keV X ray, which is the basis for the EDS and WDS techniques used in the SEM. Most of the time, however, it is relieved by the ejection of another $L_{2,3}$ shell electron that overcomes its 0.1-keV binding energy and carries off the remaining 1.6 keV of energy. This characteristic energy is the basis for the identification of this electron as having come from a Si atom in the sample. This electron is called a Si $KL_{2,3}L_{2,3}$ Auger electron and the process is called a KLL Auger transition. This process leaves the atom with 2 vacancies in the $L_{2,3}$ shell that may further decay by Auger processes involving

electrons from the Si M shell, which is also the valence band, and thus these Auger transitions are called LVV transitions. The two valence-band electrons involved in an LVV transition may come from any two energy states in the band, although they will most probably come from near peaks in the valence-band density of states, and thus the shape of the LVV "peak" is derived from a self convolution of the valence-band density of states, and the width of the LVV peak is twice the width of the valence band.

The complete description of the number of Auger electrons that are detected in the energy distribution of electrons coming from a surface under bombardment by a primary electron beam contains many factors. They can be separated into contributions from four basic processes, the creation of inner shell vacancies in atoms of the sample, the emission of electrons as a result of Auger processes resulting from these inner shell vacancies, the transport of those electrons out of the sample, and the detection and measurement of the energy distribution of the electrons coming from the sample.

In fact, Auger electrons are generated in transitions back to the ground state of atoms with inner shell vacancies, no matter what process produced the inner shell vacancy. Auger peaks are therefore observed in electron energy spectra generated by electron excitation, X-ray excitation, and ion excitation, as well as in certain nuclear reactions. The technique usually referred to as Auger electron spectroscopy uses excitation by an electron beam. The spectra produced by X-ray excitation in XPS routinely also include Auger peaks mixed in with the photoelectron peaks. Ion beam-induced Auger peaks occur, at times, during the depth profiling mode of analysis in AES.

Production of Inner Shell Vacancies

The probability (cross section) that a high-energy incident electron will produce a particular inner shell vacancy in a certain element is a function of the ratio of the primary electron energy to the binding energy of the electrons in that shell. In general the cross section rises steeply from 0 at a ratio of 1 to a maximum at a ratio in the range from 3 to 6 and then decreases gradually as the ratio increases further. As an example, the Si K shell binding energy is 1844 eV. To get the maximum yield of Si K shell vacancies, and therefore Si KLL Auger electrons, a primary electron-beam energy of 5.5–11.0 keV should be used. On the other hand if better surface sensitivity is needed (see below) the low-energy Si LVV transition is preferred. The Si L shell binding energies are 154 and 104 eV, so the primary beam energy would be optimized at 0.3–0.9 keV for these transitions.

Auger Electron Emission

Once an inner shell vacancy is created in an atom the atom may then return toward its ground state via emission of a characteristic X ray or through a radiationless Auger transition. The probability of X-ray emission is called the fluorescence yield.
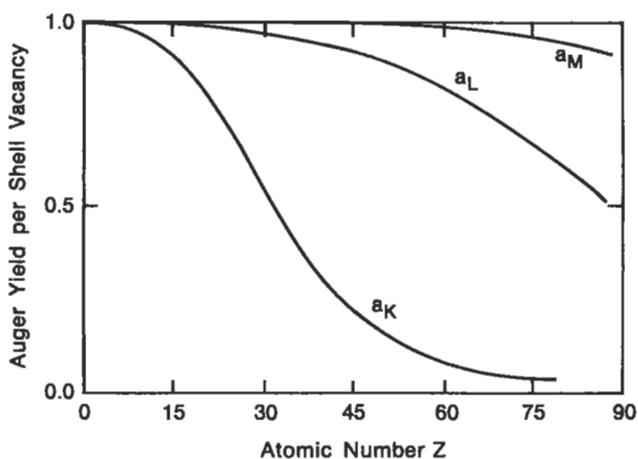
Figure 2   **Percentage of inner shell vacancies resulting in Auger electron emission for holes in the K, L, and M shells.**

The Auger yield is 1 minus the fluorescence yield, since these are the only two options. Figure 2 shows the Auger yield as a function of atomic number for initial vacancies in the K, L, and M shells. It is clear that Auger emission is the preferred decay mechanism for K shell vacancies in the low atomic number elements, and for L and M shell initial vacancies for all elements. By properly selecting the Auger transition to monitor, all elements (except H and He) can be detected using Auger transitions that have a 90% or higher Auger yield per initial vacancy.

Electron Transport to the Surface

As the various electrons, including Auger electrons, resulting from primary electron bombardment diffuse through the sample and to the surface many scattering events occur. The inelastic collisions have the effect of smoothing the energy distribution of these electrons and result in a power law energy distribution[4] at energies between the elastic peak and the "true secondary" peak, which occur at the high-energy and low-energy end of the distribution, respectively. This produces a background, as shown in Figure 1b, on which the Auger peaks are superimposed, that can be modeled and removed (see below). Inelastic collisions also have the effect of removing some of the Auger electrons from their characteristic energy position in an Auger peak and transferring them to lower energies as part of the "loss tail," which starts at the low-energy side of the Auger peak and extends all the way to zero energy.

The inelastic collision process is characterized by an inelastic mean free path, which is the distance traveled after which only $1/e$ of the Auger electrons maintain their initial energy. This is very important because only the electrons that escape the sample with their characteristic Auger energy are useful in identifying the atoms in

the sample. This process gives the technique its surface specificity. This inelastic mean free path is a function, primarily, of the energy of the electron and, secondarily, of the material through which the electron is traveling. Figure 6 in the XPS article shows many measurements of the inelastic mean free path in various materials and over a wide range of energies, and an estimate of a universal (valid for all materials) inelastic mean free path curve versus energy.

The minimum in the mean free path curve, at around 80 eV, is the energy at which electrons travel the shortest distance before suffering an energy-altering scattering event. Thus Auger electrons that happen to have their energy in this vicinity will be those that will have the thinnest sampling depth at the surface. For example, while Si LVV Auger electrons from oxidized Si (at approximately 78-eV) are generated at depths ranging from the top monolayer to nearly a μm from a primary electron beam with a typical 5-keV energy, 63% of the electrons that escape without losing any energy come from the top 5 Å of the sample. Furthermore, 87% are contributed by the top 10 Å of the sample and 95% have been produced in the top 15 Å of material. The depth from which there is no longer any signal contribution is ultimately determined by the signal-to-noise ratio in the measured spectrum. If a 5% signal variation is accurately measurable then atoms 3 mean free paths down contribute to the measurement. If 2% of the signal is well above the noise level then atoms at a depth of 4 mean free paths contribute to the measurement.

Secondary Electron Collection

As the electrons leave the surface they move in a cosine-shaped intensity distribution away from the analysis point and travel in straight lines until they enter the energy analyzer. The entrance slit of the energy analyzer determines the percentage that are collected, but it is typically just under 20% for the most commonly used energy analyzer, the cylindrical mirror analyzer (CMA). Once in the energy analyzer more electrons are lost by scattering at grids and the CMA transmission is typically 60%.

Information in Auger Spectra

Using the best procedures during data acquisition produces spectra with the maximum available information content. Once spectra are recorded that contain the information that is sought using the best procedures for extracting the information from the data is important to maximize the value of the analysis. This section will consider the procedures for data acquisition and the extraction of various types of information available from the data.

Data Acquisition

For primarily historical reasons people have come to consider Auger spectra as having the form, $dN(E)/dE$ versus E, where $N(E)$ is the energy distribution of the sec-
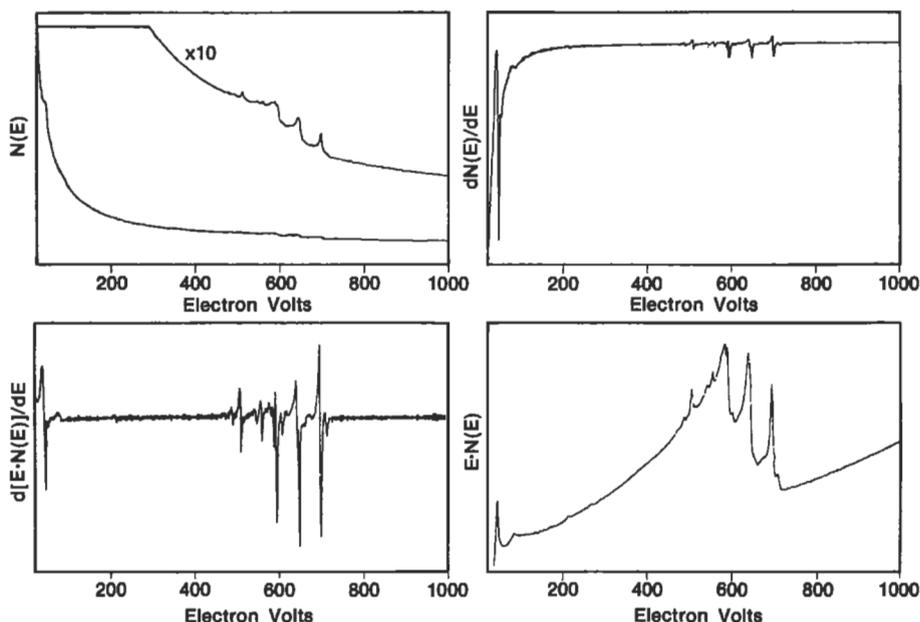
Figure 3   The $N(E)$, $dN(E)/dE$, $dEN(E)/dE$, and $EN(E)$ forms of secondary electron energy spectra from a slightly contaminated Fe surface.

ondary electrons being detected and E is their energy. This came about because of the properties of various energy analyzers used and because of peculiarities of the analog electronics used to run them. Spectra in this form were acquired by adding an AC component to the energy-selecting voltage of the energy analyzers (a modulation) and detecting the signal with a lock-in amplifier.[5] This led to the signal being acquired in the differential mode, $dN(E)/dE$ versus E, instead of $N(E)$ versus E. These forms of acquired spectra are shown in Figure 3. With the advent of the CMA and computer-controlled digital signal acquisition, which can be coupled with either pulse counting or voltage-to-frequency conversion for decoupling the signal from the high positive collection voltage, it has finally become practical to discard the modulation and the lock-in amplifier in signal acquisition, as is done in Figure 3(bottom right panel). Acquiring data directly in $N(E)$ (or $E \times N(E)$) form, followed by subsequent mathematical processing, provides six valuable advantages:

1   There is an improved signal-to-noise ratio in the raw data. This can be seen in the $E \times N(E)$ form of data in Figure 3.

2   The energy analyzer is always operated at its best energy resolution.

3   The measured Auger signal is proportional to the number of atoms sampled. In the derivative mode of data acquisition this is frequently not the case, for example, if an inappropriate modulation voltage is used or if the line shape has

changed due to a change in chemical environment.

4 The physical information in the line shape is immediately available for observation.

5 Peak overlaps can be eliminated simply by peak fitting and subtraction.

6 Loss tail analysis can be applied to the data. (This procedure is discussed below.)

Thus it is best to acquire and store the data in the simplest and least-processed form possible.

Extracting Information From the Data

There are at least four kinds of information available from an Auger spectrum. The simplest and by far most frequently used is qualitative information, indicating which elements are present within the sampling volume of the measurement. Next there is quantitative information, which requires a little more care during acquisition to make it extractable, and a little more effort to extract it, but which tells how much of each of the elements is present. Third, there is chemical information which shows the chemical state in which these elements are present. Last, but by far the least used, there is information on the electronic structure of the material, such as the valance-band density of states that is folded into the line shape of transitions involving valance-band electrons. There are considerations to keep in mind in extracting each of these kinds of information.

Qualitative Information

Qualitative information can be extracted from Auger spectra quite simply, by a trained eye or by reference to one of the available Auger charts, tables of energies, or handbooks of spectra. The most basic identification is done from the energies of the major peaks in the spectrum. The next level of filtration is done from the peak intensity ratios in the patterns of peaks in the spectra of the elements present. One of the charts of Auger peak energies available is shown in Figure 4. The useful Auger spectra of the elements fall into groups according to the transition type, KLL, LMM, MNN, etc. If you look across the chart, following a given energy, it is clear that there are many possibilities for intermixing of patterns from different elements, but there are few direct peak overlaps. Generally, if there are peaks from two elements that interfere, there are other peaks from both those elements that do not overlap. One of the most difficult exceptions to this rule is in the case of B and Cl: B has only one peak, a KLL peak at 180 eV. Cl has an LMM peak at 180 eV and its KLL peaks are at 2200–2400 eV, high enough that they are seldom recorded. If there is a real uncertainty as to which of these elements is present, it is necessary to look for the latter peaks.

Peak overlaps that totally obscure one of the elements in the spectrum have been shown to be separable.[6] A Co–Ni alloy film under a Cu film is a combination that produces a spectrum where the Ni peaks are all overlapped by Cu or Co peaks, or
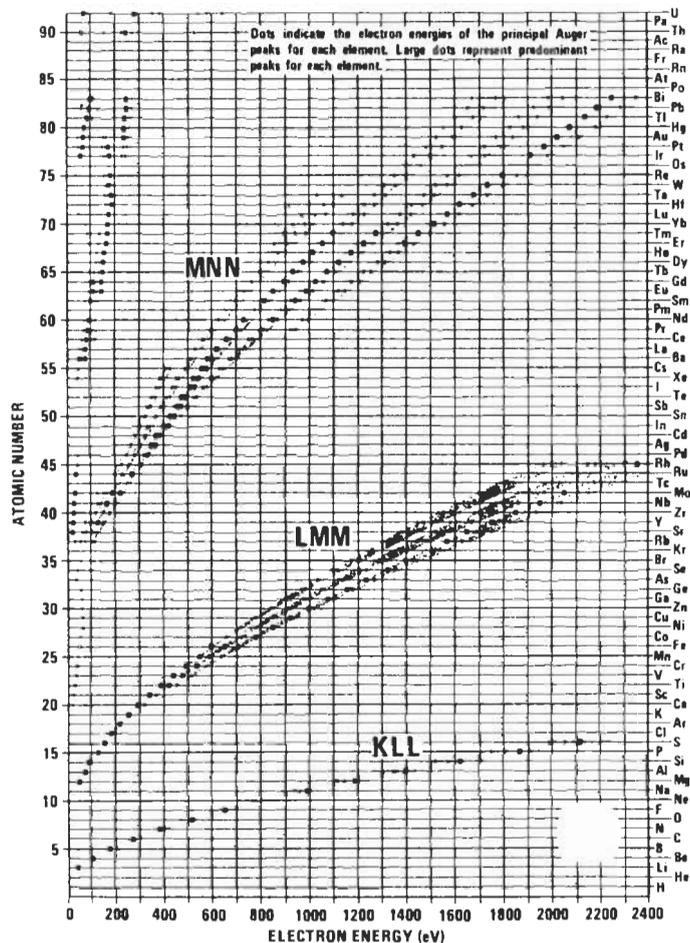
Figure 4 One of the numerous available charts of Auger electron energies of the elements.

both. The intensities in the Cu and Co patterns show that another element is present. With the use of background subtraction, standard spectra, and peak fitting and subtraction, the Ni spectrum was uncovered and identified, and even quantitative information, with identified accuracy limitations, was obtained.

When listing the elements present from qualitative analysis, the issues of sensitivity and signal-to-noise level arise. The minimum amount of an element that must be present to be detected in an Auger spectrum is a function of a number of variables. Some of these are determined by the element, such as its ionization cross section at the primary energy being used, the Auger yield from its most prolific inner shell vacancy, the energy of its Auger electron (since this determines the elec-

trons' mean free path for escape from the solid), etc. Other variables are under the control of the measurement parameters, such as the primary beam energy and current, the energy resolution of the energy analyzer, the angle of incidence of the primary beam onto the sample and the acceptance angle of the energy analyzer. These variables can, to a certain degree, be controlled to yield the maximum signal-to-noise ratio for the element of interest. When these parameters are optimized the detection limit for most elements is on the order of a few times $10^{18}/\text{cm}^3$ homogeneously distributed, or about 1 atom in 10,000.

Quantitative Information

The number of Auger electrons from a particular element emitted from a volume of material under electron bombardment is proportional to the number of atoms of that element in the volume. However it is seldom possible to make a basic, first principles calculation of the concentration of a particular species from an Auger spectrum. Instead, sensitivity factors are used to account for the unknown parameters in the measurement and applied to the signals of all of the species present which are then summed and each divided by the total to calculate the relative atomic percentages present.

Of the total number of Auger electrons emitted only a fraction escapes the sample without energy loss. The rest become part of the loss tail on the low-energy side of the Auger peak extending to zero energy and contribute to the background under all of the lower energy Auger peaks in the spectrum. This process must be taken into account when using a sensitivity factor for a particular Auger system. Sensitivity factors are usually taken from pure elemental samples or pure compound samples. This means that the element is homogeneously distributed in the standard. If this is not true in the unknown sample, the percentage of Auger electrons that escape the sample without energy loss changes. If the element is concentrated at the surface, fewer Auger electrons will suffer energy loss; if it is concentrated in a layer beneath another film, more Auger electrons will suffer energy loss before they escape the sample. This can be seen in Figure 5, which shows oxygen in a homogeneous SiO_2 film, in a surface oxide on Si, and from an SiO_2 film under a layer of Si. An oxygen sensitivity factor determined from a homogeneous sample would not properly represent the oxygen concentration in the lower two spectra of Figure 5.

Sensitivity factors should be measured on the same energy analyzer, at the same energy resolution, at the same primary electron beam energy, and at the same sample orientation to the electron beam and energy analyzer, as the spectra to which they are applied. Only when these precautions are taken can any sort of quantitative accuracy be expected. Even with these precautions the oxygen example discussed above and shown in Figure 5 would present a problem. The most direct way to prevent this problem is by the process referred to above as "loss tail analysis." This involves comparing the ratios of the peak heights to the loss tail heights, on background subtracted spectra, from the spectrum of the unknown sample and the
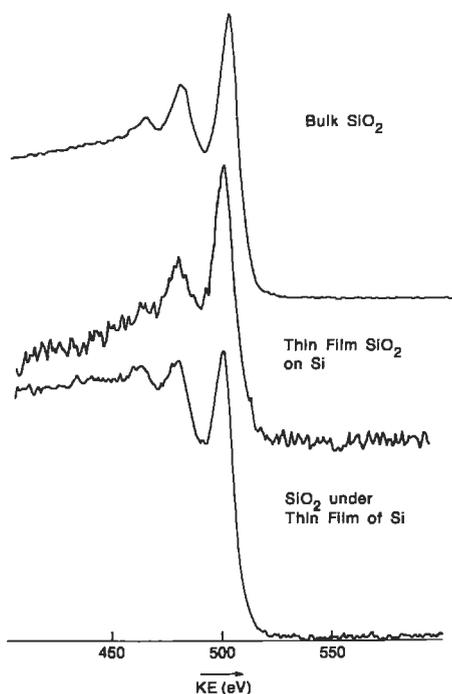
Figure 5 Oxygen spectra from bulk SiO_2, a thin film of SiO_2 on Si, and SiO_2 under a thin film of Si. These spectra have had their background removed, and so the loss tail can be seen as the height of the spectra at energies below the peaks.

spectrum from which the sensitivity factor was determined. When these ratios are equal the same degree of depth homogeneity of the element in question is assured.

Chemical Information

There is a great deal of chemical information in the line shapes and chemical shifts of peaks in Auger spectra. XPS is generally considered to be a more appropriate tool to determine chemistry in a sample. It is true that the photoelectron lines used in XPS are typically narrower and that therefore smaller chemically induced energy shifts can be detected. Moreover, the energy analyzers used in XPS often have better energy resolution. However, it is also true that the chemically induced energy shifts in Auger peaks are usually larger than the corresponding shifts in photoelectron peaks.[7]

Chemical information is present in Auger spectra in two forms; a shift in the energy of the peak maximum and sometimes as a change in the line shape of the Auger peak. Line shape changes are greatest in transitions involving valance-band electrons, such as the LVV transition in Si. Since this line shape is just a weighted